Dynamic control of higher-order modes in hollow-core photonic crystal fibers

T. G. Euser[1], G. Whyte[3], M. Scharrer[1], J. S. Y. Chen[1], A. Abdolvand[1], J. Nold[1], C. F. Kaminski[1,2,3] and P. St.J. Russell[1]

[1]Max-Planck Research Group (IOIP), University of Erlangen-Nuremberg
Guenther-Scharowsky Str. 1/Bau 24, 91058 Erlangen, Germany
[2]SAOT - Erlangen Graduate School in Advanced Optical Technologies
[3]Department of Chemical Engineering, University of Cambridge,
Pembroke Street, Cambridge CB2 3RA, UK
www.pcfiber.com

Abstract: We present a versatile method for selective mode coupling into higher-order modes of photonic crystal fibers, using holograms electronically generated by a spatial light modulator. The method enables non-mechanical and completely repeatable changes in the coupling conditions. We have excited higher order modes up to LP_{31} in hollow-core photonic crystal fibers. The reproducibility of the coupling allows direct comparison of the losses of different guided modes in both hollow-core bandgap and kagome-lattice photonic crystal fibers. Our results are also relevant to applications in which the intensity distribution of the light inside the fiber is important, such as particle- or atom-guidance.

OCIS codes: (060.5295) Photonic crystal fibers; (230.6120) Spatial light modulators

References and links

1. P. St.J. Russell, "Photonic crystal fibers," J. Lightwave Technol. **24**, 4729-4749 (2006), http://www.opticsinfobase.org/JLT/abstract.cfm?URI=JLT-24-12-4729.
2. R. F. Cregan, B. J. Mangan, J. C. Knight, T. A. Birks, P. St.J. Russell, P. J. Roberts, and D. C. Allan, "Single-mode photonic band gap guidance of light in air," Science **285**, 1537-1539 (1999), http://www.sciencemag.org/cgi/content/abstract/285/5433/1537.
3. F. Couny, F. Benabid, and P. S. Light, "Large-pitch kagome-structured hollow-core photonic crystal fiber," Opt. Lett. **31**, 3574-3576 (2006), http://www.opticsinfobase.org/abstract.cfm?URI=ol-31-24-3574.
4. A. Argyros and J. Pla, "Hollow-core polymer fibres with a kagome lattice: potential for transmission in the infrared," Opt. Express **15**, 7713-7719 (2007), http://www.opticsinfobase.org/abstract.cfm?URI=oe-15-12-7713.
5. G. J. Pearce, G. S. Wiederhecker, C. G. Poulton, S. Burger, and P. St.J. Russell, "Models for guidance in kagome-structured hollow-core photonic crystal fibres," Opt. Express **15**, 12680-12685 (2007), http://www.opticsinfobase.org/abstract.cfm?URI=oe-15-20-12680.
6. F. Benabid, F. Couny, J. C. Knight, T. A. Birks, and P. St.J. Russell, "Compact, stable and efficient all-fibre gas cells using hollow-core photonic crystal fibres," Nature **434** 488-491 (2005), http://www.nature.com/nature/journal/v434/n7032/abs/nature03349.html.
7. F. Benabid, J. C. Knight, and P. St.J. Russell, "Particle levitation and guidance in hollow-core photonic crystal fiber," Opt. Express 10, 1195-1203 (2002), http://www.opticsinfobase.org/abstract.cfm?URI=oe-10-21-1195 .
8. F. Benabid, P. S. Light, F. Couny, and P. St.J. Russell, "Electromagnetically-induced transparency grid in acetylene-filled hollow-core PCF," Opt. Express **13**, 5694-5703 (2005), http://www.opticsinfobase.org/abstract.cfm?URI=oe-13-15-5694.
9. S. Ghosh, A. R. Bhagwat, C. K. Renshaw, S. Goh, A. L. Gaeta, and B. J. Kirby, "Low-light-level optical interactions with rubidium vapor in a photonic bandgap fiber," Phys. Rev. Lett. 97 023603 (2006), http://link.aps.org/abstract/PRL/v97/e023603.
10. E. A. J. Marcatili, and R. A. Schmeltzer, "Hollow metallic and dielectric waveguides for long distance optical transmission and lasers," Bell. Sys. Tech. J. **43**, 1783-1809 (1964).
11. A. A. Ishaaya, B. Shim, C. J. Hensley, S. E. Schrauth, A. L. Gaeta, and K. W. Koch, "Efficient excitation of polarization vortices in a photonic bandgap fiber with ultrashort laser pulses," in *Conference on Lasers and*

#101362 - $15.00 USD Received 8 Sep 2008; revised 17 Oct 2008; accepted 19 Oct 2008; published 21 Oct 2008

Electro-Optics/Quantum Electronics and Laser Science and Photonic Applications Systems Technologies, Technical Digest (CD) (Optical Society of America, 2008), paper CThV3, http://www.opticsinfobase.org/abstract.cfm?URI=CLEO-2008-CThV3.

12. Y. Yirmiyahu, A. Niv, G. Biener, V. Kleiner, and E. Hasman, "Excitation of a single hollow waveguide mode using inhomogeneous anisotropic subwavelength structures," Opt. Express **15**, 13404-13414 (2007), http://www.opticsinfobase.org/oe/abstract.cfm?URI=oe-15-20-13404.
13. V. R. Daria, P. J. Rodrigo, and J. Gluckstad, "Programmable complex field coupling to higher-order guided modes of micro-structured fibres," Opt. Comm. **232**, 229-237 (2004), doi:10.1016/j.optcom.2003.12.075.
14. T. Pfeifer, R. Kemmer, R. Spitzenpfeil, D. Walter, C. Winterfeldt, G. Gerber, and C. Spielmann, "Spatial control of high-harmonic generation in hollow fibers," Opt. Lett. **30**, 1497-1499 (2005), http://www.opticsinfobase.org/abstract.cfm?URI=ol-30-12-1497.
15. D. Walter, T. Pfeifer, C. Winterfeldt, R. Kemmer, R. Spitzenpfeil, G. Gerber, and C. Spielmann, "Adaptive spatial control of fiber modes and their excitation for high-harmonic generation," Opt. Express **14**, 3433-3442 (2006), http://www.opticsinfobase.org/abstract.cfm?URI=oe-14-8-3433.
16. J. Liesener, M. Reicherter, T. Haist, and H. J. Tiziani, "Multi-functional optical tweezers using computer-generated holograms," Opt. Comm. **185**, 77-82 (2000), doi:10.1016/S0030-4018(00)00990-1.
17. J. E. Curtis, B. A. Koss, and D. G. Grier, "Dynamic holographic optical tweezers," Opt. Comm. **207**, 169-175 (2002), doi:10.1016/S0030-4018(02)01524-9.
18. G. Whyte, G. Gibson, J. Leach, M. Padgett, D. Robert, and M. Miles, "An optical trapped microhand for manipulating micron-sized objects," Opt. Express **14**, 12497-12502 (2006), http://www.opticsinfobase.org/abstract.cfm?URI=oe-14-25-12497.
19. G. Whyte, and J. Courtial, "Experimental demonstration of holographic three-dimensional light shaping using a Gerchberg-Saxton algorithm," New J. Phys. **7**, 1-12 (2005), doi:10.1088/1367-2630/7/1/117.
20. P. J. Roberts, D. P. Williams, H. Sabert, B. J. Mangan, D. M. Bird, T. A. Birks, J. C. Knight, P. St.J. Russell, "Design of low-loss and highly birefringent hollow-core photonic crystal fiber," Opt. Express **14**, 7329-7341 (2006), http://www.opticsinfobase.org/oe/abstract.cfm?URI=oe-14-16-7329.
21. A. Argyros, S. G. Leon-Saval, J. Pla, and A. Docherty, "Antiresonant reflection and inhibited coupling in hollow-core square lattice optical fibres," Opt. Express **16**, 5642-5648 (2008), http://www.opticsinfobase.org/abstract.cfm?URI=oe-16-8-5642.
22. M. J. Booth, "Adaptive optics in microscopy," Philos. Transact. A Math. Phys. Eng. Sci. **365**, 2829-2843 (2007), doi:10.1098/rsta.2007.0013.

1. Introduction

The often unique properties offered by photonic crystal fibers (PCFs) have created many opportunities for studying the interaction between matter and intense light fields [1]. In particular, hollow-core (HC) PCFs [2] are being exploited for their ability to maximize the interaction of light and low-refractive-index samples at path-lengths that are much longer than achievable in conventional single-pass cells. In HC-PCFs, guidance is achieved through two mechanisms. In the first, the creation of one or more photonic bandgaps in the microstructured cladding allows formation of low-loss guided modes within certain wavelength ranges where a core resonance coincides with a bandgap. In contrast, in HC-PCFs with a kagome lattice in the cladding [3,4] the guidance mechanism is not based on bandgaps, but rather on reduced coupling between the core-mode and cladding-modes [4,5]. In this Letter we refer to these two types of HC-PCF as HC-bandgap and HC-kagome fibers. HC-PCFs have very significantly enhanced a range of different light-matter interactions, for example, stimulated Raman scattering in hydrogen [6], particle guidance [7] and electromagnetically induced transparency in acetylene [8, 9].

Bound modes appear in waveguides when the fields in the cladding are evanescent, i.e., there are no real photonic states. In absorption-free waveguides, such modes will exhibit a loss that falls exponentially as the cladding thickness increases. This happens in hollow core PCF when the cladding supports a photonic band gap, under which circumstances the attenuation falls exponentially as more and more periods are added to the cladding. In leaky waveguides, however, there are always real states (i.e., propagating fields) in the cladding, so that Fabry-Pérot like resonances appear in the cladding, the leakage rate depending in a complicated oscillatory manner on cladding thickness as well as on the properties of the

#101362 - $15.00 USD Received 8 Sep 2008; revised 17 Oct 2008; accepted 19 Oct 2008; published 21 Oct 2008

external medium. This is the case in HC-kagome fibers, where there are always real states in the cladding, making the leaky core mode look more like a Mie resonance than a bound mode. HC-kagome fibers typically also have larger core diameters, allowing them to support several such leaky resonances or "modes".

The modal field patterns in HC-PCF are similar to those seen in hollow capillary waveguides [10]. Coupling into these modes is usually performed by splicing to a standard single-mode fiber, or by butt-coupling. While allowing high launch efficiencies over a broad wavelength range, and avoiding the effects of chromatic aberration in the coupling objective, these techniques result in uncontrolled excitation of many different core and cladding modes.

Recently it was shown that higher-order modes can be efficiently excited in HC-bandgap fibers by means of higher-order Gaussian beams prepared using fixed phase-plates [11]. Excitation of a variety of single higher-order modes in a hollow metallic waveguide with a 300 μm bore at wavelength λ = 10.6 μm has been demonstrated using static diffractive elements, each mode requiring a separate element [12]. Adaptive coupling to double-lobed modes in solid-core PCFs has also been reported, using simple electronically switchable binary gratings [13]. In hollow capillaries, spatial light modulators with feedback loops based on genetic algorithms have been applied to optimize high-harmonic generation [14,15]. In such experiments, many different waveguide modes are simultaneously excited, their relative phases being adjusted so that a desired intensity distribution is reached at the fiber end-face. Since this optimization process involves many fiber modes propagating at different phase velocities, the transverse intensity distribution will vary strongly along the capillary.

In this Letter we report efficient launching of light into selected guided modes by controlling the intensity and phase distribution at the input face using a dynamic holographic technique, similar to that used in optical tweezer experiments [16-19]. An electronically-addressable spatial light modulator (SLM) is used to generate pure Hermite-Gaussian (HG) and Laguerre-Gaussian (LG) beams, which serve as an approximation to the modes in HC-PCF [10]. The set-up allows dynamic changes to be rapidly made between different modes, without mechanical realignment. Throughout the paper we have adopted the LP (linearly polarized) notation to label the different guided modes.

2. Experimental details

2.1 Holographic setup for generation of Laguerre-Gaussian beams

Figure 1 shows a schematic of the set-up used. The continuous wave Nd:YAG laser used (λ = 1064 nm, 4 W, Coherent Compass 1064-4000m) oscillated in the TEM_{00} mode with a long-term power stability better than 0.6%. The polarization state was rotated with a half-wave plate, and the beam was then attenuated and expanded from 4 mm to 20 mm to ensure homogeneous illumination of the SLM. The intensity across the SLM was measured to be constant within 10% of its maximum value. The SLM used was a high-resolution (1920×1080 pixels) liquid crystal-on-silicon (LCOS) active-matrix reflective-mode phase-only liquid crystal display, optimized for operation at λ = 1064 nm (Holoeye Pluto NIR). We used it in its electrically-controlled birefringence mode, which produces phase-only modulation. The relative phase-delay for each pixel could be changed from 0 to 2π.

The throughput from the beam expander (BE) to the aperture (A) was estimated to be 2%, mainly due to overfilling of the SLM and to beam-splitter losses. We estimate that this could be increased to 40% by removing the beam expander and the BS, at the same time slightly tilting the SLM. Such improved throughput would allow this technique to be extended to higher power applications.

#101362 - $15.00 USD Received 8 Sep 2008; revised 17 Oct 2008; accepted 19 Oct 2008; published 21 Oct 2008

The SLM surface is placed in the front Fourier plane of lens L1 and thus acts as a hologram. Each point source P in the SLM plane gives rise to a uniform plane-wave whose wavevector is parallel to the line from P to the centre of the lens. The hologram shapes the light beam in a volume around the back Fourier plane of lens L1. The phase pattern required to generate a certain intensity distribution is calculated via a Fourier transform. A blazed diffraction grating directs the shaped beam towards the +1 diffracted order, as schematically shown in Fig. 1(b). The other orders, caused by imperfections in the phase response of the SLM, are filtered out by the Fourier-plane aperture A [19]. The orientation and period of the grating can be electronically adjusted accurately to control the direction of the diffracted beam.

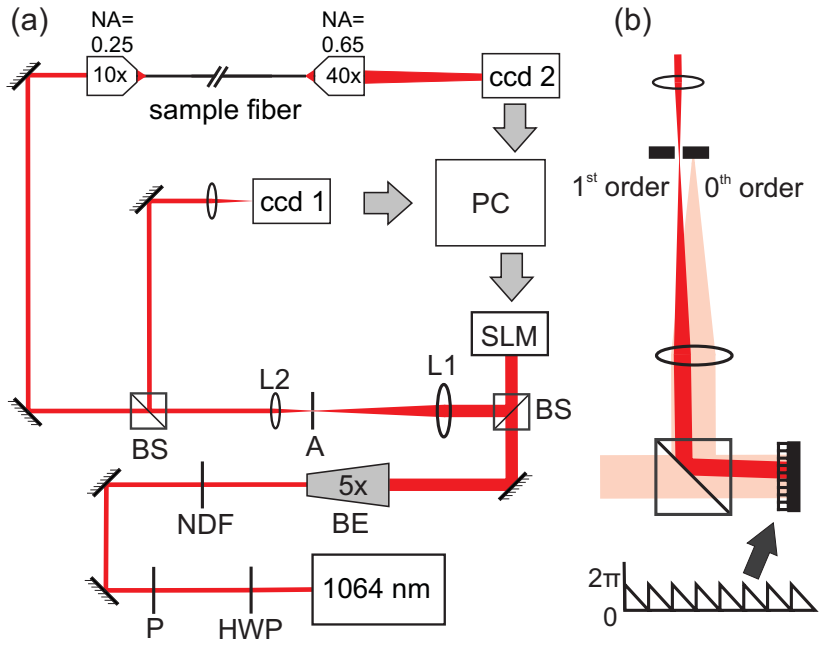

Fig. 1. Experimental set-up. (a) A 1064 nm laser beam is expanded 5× so as to homogeneously fill the spatial light modulator (SLM). The SLM is placed in the front Fourier plane of lens L1 (focal length 30 cm). It shapes the light beam in a volume around the back Fourier plane of lens L1. A second lens L2 (focal length 5 cm) is used to compress and collimate the modulated beam. Part of the beam is reflected to a CCD camera (CCD 1) for online monitoring of the generated intensity profiles. A 10×0.25 NA microscope objective is used to couple the beam into the sample fiber. The end-face of the fiber is imaged on to a second camera (CCD 2) using a 40×0.65 NA objective. HWP: half wave plate; P: polarizer; NDF: neutral density filter; BE: 5× beam expander; BS: beam splitter; L1 and L2: lenses; PC: computer. (b) A blazed phase grating is used to redirect the shaped beam into the +1 diffracted order, the other orders being filtered out using a Fourier-plane aperture A.

After the aperture, the beam is collimated by lens L2 to a diameter of ~1.6 mm. Part of the beam is directed towards the sample fiber, and part of it is reflected towards the camera CCD1, which images the intensity profile of the beam. Three examples of higher-order LG and HG modes generated by the set-up are shown in Fig. 2. The target intensities are shown in the left column, the holograms applied to the SLM in the middle and the measured intensity profiles on the right. The modes shown are the LG_{01} mode, the radial HG_{01} mode and the radial HG_{02} mode. We find good agreement between the target and measured intensity distributions. The orientation of the modes can be dynamically adjusted by changing the orientation of the hologram.

#101362 - $15.00 USD Received 8 Sep 2008; revised 17 Oct 2008; accepted 19 Oct 2008; published 21 Oct 2008

For efficient coupling into HC-PCF, it is essential to have control over as many coupling parameters as possible. In our system, the coupling conditions could be adjusted electronically by changing the hologram on the SLM. In the current setup, shown in Fig. 1, the in-coupling position can be varied in sub-micron steps over a range of ±80 μm, by changing the orientation and period of the blazed grating. Furthermore, the size of the beam, and thus the effective numerical aperture (NA), can be adjusted by rescaling the size of the hologram. Importantly, the in-coupling angle of the beam can be independently controlled by changing the position of the hologram on the SLM surface. The coupling angle can be adjusted within a cone with radius of 50 mrad, with a step-size of 85 μrad. We note that this range can easily be extended by choosing a different (higher-NA) coupling objective.

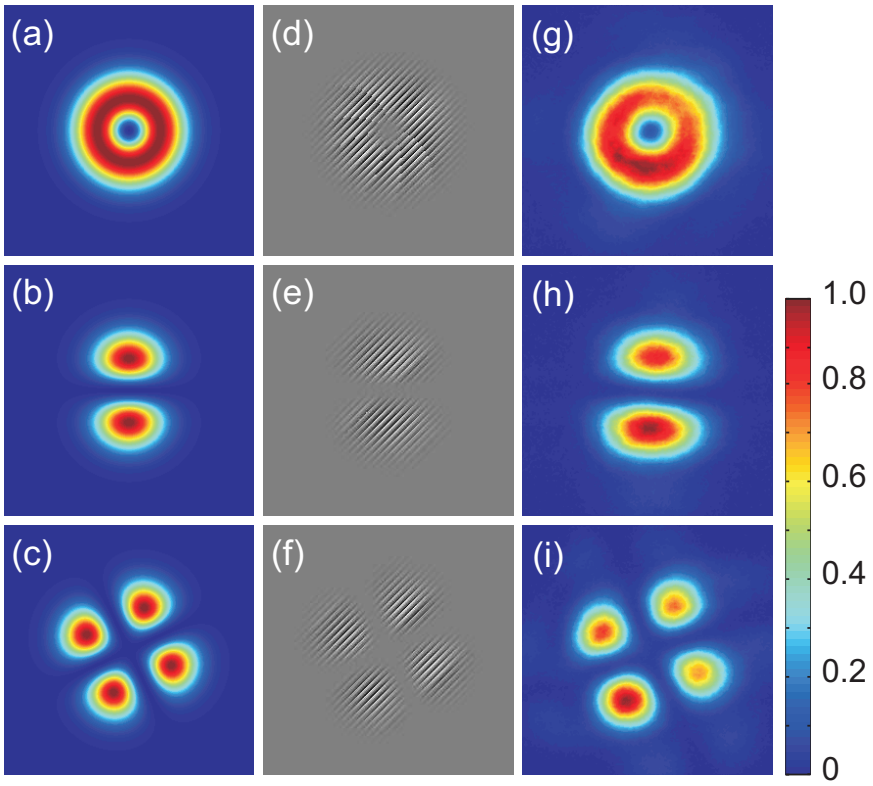

Fig. 2. (a-c) Normalized target intensity distributions for LG_{01} mode (a) radial HG_{01} mode (b) radial and HG_{02} mode (c); (d-f) corresponding holograms generated by the SLM (black is 0, white is 2π); (g-i) resulting normalized intensity distribution measured by CCD1.

2.2 Hollow-core photonic crystal fibers

The hollow-core PCFs used in the experiments were fabricated using the conventional stack-and-draw process. Silica tubes were first drawn to thin-walled capillaries of the desired diameter. The capillaries were stacked and inserted into a jacket tube to create a preform, which was then drawn down to a cane. Different pressures were applied to the core and cladding regions of the cane to allow independent control of core-diameter and air-filling fraction in the cladding. Fig. 3(a) shows a scanning electron micrograph (SEM) of the microstructure of the HC-bandgap fiber. The cladding crystal has a pitch of 3.2±0.1 μm and the core diameter is 12.0±0.2 μm. Fig. 3(c) shows a near-field optical micrograph of the light emerging from a 3 cm length of HC-kagome fiber with pitch 11.9±0.2 μm and core diameter

#101362 - $15.00 USD Received 8 Sep 2008; revised 17 Oct 2008; accepted 19 Oct 2008; published 21 Oct 2008

23.4±0.2 µm. The strut width was measured from high-resolution SEMs and is 325±25 nm in the core surround and lies between 350 nm and 450 nm in the rest of the cladding cladding. The fiber was illuminated from below with a halogen lamp. The colors observed in the air-holes in the cladding are related to their differing diameters, and are caused by long-lived Mie-like resonances.

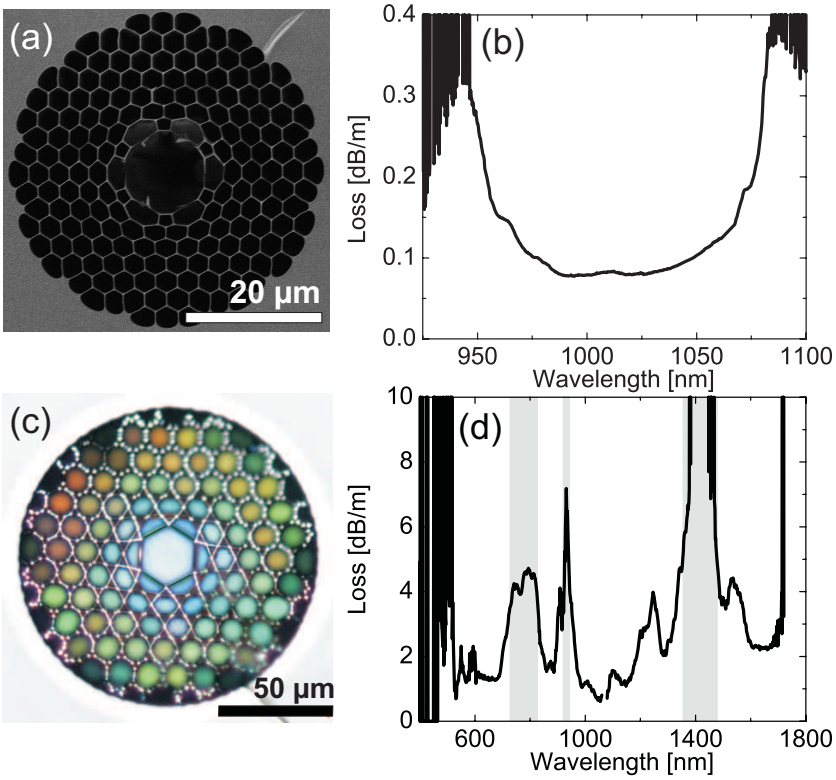

Fig. 3. Micrographs and loss spectra of the fibers used in our experiments: (a) SEM of the cross-section of the HC-bandgap fiber with pitch Λ = 3.2±0.1 µm and core diameter d_{core}= 12.0±0.2 µm; (b) loss spectrum of the fiber shown in (a); (c) optical micrograph of the near-field emerging from a 3 cm long piece of HC-kagome PCF with pitch Λ= 11.9±0.2 µm and d_{core}= 23.4±0.2 µm, illuminated from below with a halogen lamp. The thickness of the glass struts in the cladding varied between 350 and 450 nm; (d) loss spectrum of the fiber in (c); the shaded areas indicate measured bands of loss.

2.*3 Loss measurements*

The spectral attenuation of the fibers was measured using the conventional cut-back technique. A white-light supercontinuum (generated by pumping a length of endlessly single-mode PCF with light from a 1064 nm Nd:YAG microchip laser) was launched into the fiber and the transmitted spectrum measured. Without changing the in-coupling condition, the fiber was then cut back to a shorter length and the spectrum again measured. The loss was then calculated by comparing the two spectra. The supercontinuum was coupled into the sample fiber via an objective lens, allowing more freedom over the coupling parameters than fiber butt-coupling. Launch optimization was achieved by matching the numerical aperture (NA) of the coupling objective to that of the guided mode in the fiber. Optimum coupling for the HC-bandgap fiber was obtained with a slightly under-filled 20×0.4 NA objective, while for HC-kagome fiber, which has a larger core size and thus a smaller NA, a 4×0.1 NA objective was

#101362 - $15.00 USD Received 8 Sep 2008; revised 17 Oct 2008; accepted 19 Oct 2008; published 21 Oct 2008

used. At the end-face of the fiber, a 10×0.25 NA objective was used to collimate the transmitted light. A flip mirror allowed us to send the light either to a CCD beam profiler, imaging the end-face of the fiber, or to a multimode fiber connected to an optical spectrum analyzer. The CCD camera, in combination with interference filters, was used to verify that light was coupled only into the fundamental core mode at the optimization wavelength.

3. Results

3.1 Conventional loss spectra of hollow-core fibers

For both HC-bandgap and HC-kagome fibers, coupling was optimized for maximum transmission at 1000 nm. We confirmed that the light was guided in the fundamental mode at this wavelength. The loss-spectrum for the HC-bandgap fiber is based on a cut-back from 125 m to 13 m and is shown in Fig. 3(b). The spectrum reveals a transmission band between 950 and 1075 nm, where the losses are below 0.2 dB/m. The minimum observable loss was 0.07±0.1 dB/m at 990 nm. At λ = 1064 nm, the loss is 0.13±0.01 dB/m. For the HC-kagome fibers the bend-radius was kept constant at ~15 cm to minimize leakage losses. At wavelengths shorter than 900 nm, a small amount of the light was observed in the cladding region, along with higher-order core modes (we attribute this to chromatic aberrations in the coupling objective). The implication is that, in this wavelength range, the measurement may not represent the losses of the fundamental mode only.

The HC-kagome fiber loss spectrum was obtained by cut-back from 6.3 m to 1.3 m and is shown in Fig. 3(d). The fiber has losses below 2 dB/m between λ = 965 and λ = 1190 nm, with a loss of 0.7±0.1 dB/m at λ = 1064 nm. It shows a wide band of loss from 730 to 830 nm, which corresponds to resonances in struts close to the core (widths 375±25 nm and 350±25 nm measured from the SEM) [5,21]. The resonance at 930 nm corresponds approximately to struts 440 nm wide, which can be found further out in the cladding; this will result in weaker coupling and a narrower loss band, in agreement with the loss spectrum. The loss band at 1400 we attribute to OH absorption.

An accurate analysis of the loss spectra in HC-kagome fibers at wavelengths away from the optimization wavelength was not possible, mainly because light was easily coupled into multiple higher-order modes, whose losses could not be measured. In the following section we show how higher-order modes in HC-PCFs can be selectively excited, and compare their losses to those of the fundamental mode.

3.2 Excitation of higher-order modes in PCFs

To study which higher-order modes can be excited, the near-field intensity pattern at the end-face of the fiber was monitored by CCD2 (Fig. 1). The experimental procedure was as follows: the SLM was adjusted to generate a fundamental mode with a Gaussian intensity distribution, while angle and position were set to the center of their range. The fiber was first manually aligned to obtain coupling to the fundamental core mode. A 40× objective was used to image the end-face intensity distribution on to CCD2 with a magnification 56.5×. This fixed magnification factor allowed us to obtain an absolute length-scale for the intensity distributions shown in Fig. 4 and Fig. 5.

After initial alignment, no mechanical adjustments were made to the system. The excitation of the fundamental mode was then further optimized by electronically adjusting the coupling position, angle, mode orientation and beam size. After optimization, the settings were saved, and the optimization routine was repeated for the next mode. When the settings for all modes were saved, they were sequentially generated, while the intensity distribution for each mode was recorded by CCD2.

#101362 - $15.00 USD Received 8 Sep 2008; revised 17 Oct 2008; accepted 19 Oct 2008; published 21 Oct 2008

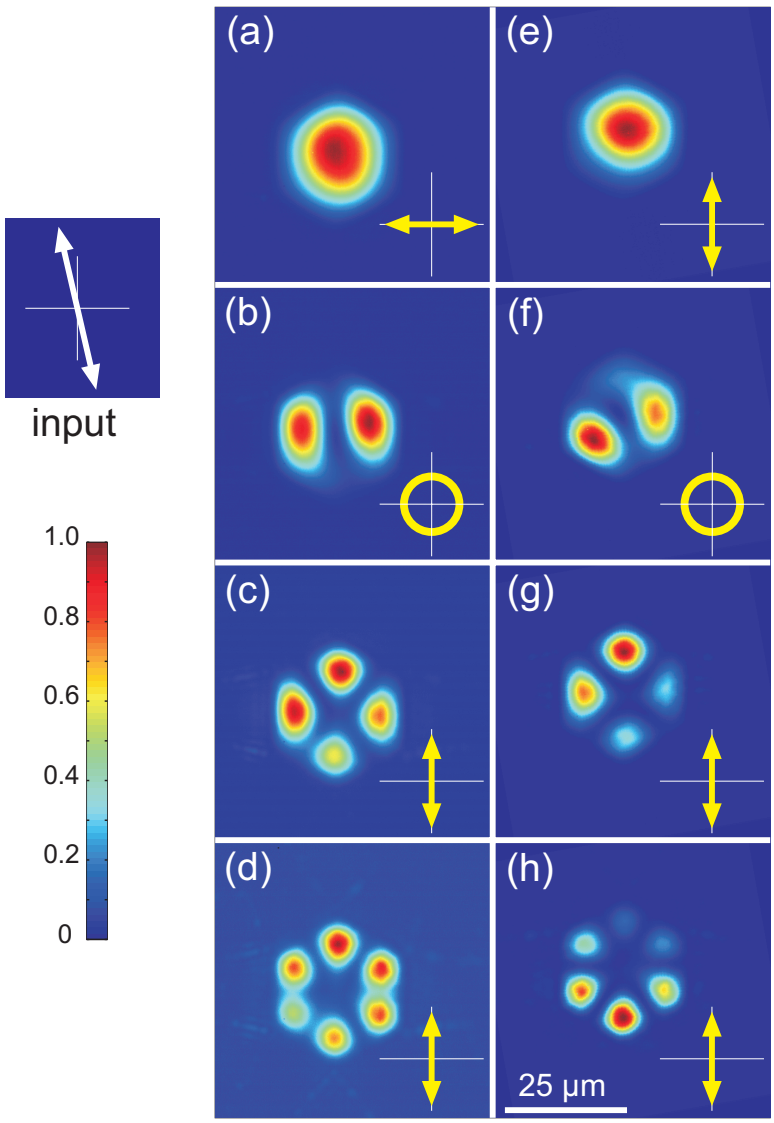

Fig. 4. Normalized near-field intensity profiles measured at the end-face of a HC-kagome fiber: (a-d) 55 cm long and (e-h) after cutback to 30 cm. The excited core resonances are: (a) fundamental LP_{01}; (b) LP_{11}; (c) LP_{21}; (d) LP_{31}. The polarization state at input to the fiber is shown on the left. The yellow arrows and circles indicate the dominant polarization state at the end-face. In (b) the transmitted signal did not change significantly as the polarizer was rotated, indicating that the light was in an elliptical polarization state (indicated by the yellow circles), and in (a) linear polarization was preserved, though it rotated slowly along the fiber, being aligned horizontally in (a) and vertically in (e).

A 55 cm length of the HC-kagome fiber shown in Fig. 3(c) was analyzed first. The fiber was kept straight to minimize bend-loss and coupling between modes. The orientation of the end-face of the fiber relative to the input-face was determined by moving the in-coupling beam into the cladding region using the SLM. The measured normalized intensity distributions at the end-face of the fiber are shown in Fig. 4. While zero (fundamental) and first-order modes have been previously observed in HC-kagome fibers [3], higher-order

#101362 - $15.00 USD Received 8 Sep 2008; revised 17 Oct 2008; accepted 19 Oct 2008; published 21 Oct 2008

modes up to LP_{31} could be excited in our set-up. In particular, the four-lobed LP_{21} mode and the six-lobed LP_{31} mode seem to be natural solutions for the hexagonally-shaped fiber core.

The fiber was next cut back to 30 cm so to allow measurement of the intensity distribution further along the fiber. After cut-back, the coupling conditions in Fig. 4(a-d) were electronically reproduced. For each core mode, the intensity profile of the shorter fiber was recorded and is shown in Fig. 4(e-h). The images were rotated to match the fiber orientation in Fig. 4(a-d). We observe that the shape and orientation of the modes remain unchanged for the LP_{01}, LP_{21} and LP_{31} modes, while the LP_{11} double-lobed mode is rotated by about 20°. Interestingly, the intensity ratio between the different lobes of the LP_{21} and LP_{31} modes has changed. We suggest that this could be caused by interactions with the glass-struts surrounding the core.

We now compare the losses of the different modes, integrating the CCD intensity profiles to obtain the total power. The LP_{01} mode had a loss of 0.55±0.10 dB/m, in good agreement with the value (0.7±0.1 dB/m) observed in the conventional loss measurement (Fig. 3(d)). The loss increases to 2.6±0.5 dB/m for the LP_{11} double-lobed mode. The highest losses however, are observed for the LP_{21} four-lobed mode (5.9±1.0 dB/m) and the LP_{31} six-lobed mode (6.6±1.3 dB/m). We conclude that higher-order modes of HC-kagome fibers suffer from elevated losses, because they interact more strongly with the cladding structure than the fundamental mode.

In all cases in Fig. 4 the input polarization was linear, aligned with the black arrow. The output polarization state for each mode was analyzed by rotating a polarizer, placed in front of CCD2, in 45° increments. The dominant polarization direction is indicated as a white arrow in each sub-figure (uncertainty ±10°). The birefringence of the fundamental mode is caused by weak interactions with the core surround, and is likely to be small [20]. As a result, the polarization state is not strongly preserved, but can rotate under the influence of random mechanical and structural perturbations. As a result, the polarization state rotates as the mode propagates along the fiber, as seen in the measurements. The LP_{11} mode was found to be in an elliptical polarization state, while the higher-order LP_{21} and LP_{31} modes maintained their input polarization. The better polarization-maintaining properties of these higher-order modes is probably due to higher birefringence, caused by stronger interactions with the glass-cladding.

We followed the same procedure to study the excitation of higher-order modes in the HC-bandgap PCF shown in Fig. 3(a). We used a 19 m long piece of fiber and first manually optimized the coupling to the fundamental mode. Next, we electronically generated and optimized the coupling to a LG_{01} beam with a doughnut-shaped intensity pattern, shown in Fig. 2(g). Fig. 5 shows the resulting normalized mode-intensity profiles at the end-face of the fiber. Both the fundamental mode and the doughnut mode showed only very small azimuthal intensity variations. We note that the linearly polarized LG_{01} beam excites a mixture of the radially and azimuthally-polarized doughnut modes [11]. The doughnut mode was also launched into a 170 m length of fiber, but the transmitted signal was too weak to be clearly distinguished from residual traces of fundamental mode.

Losses in the HC-bandgap fiber were determined by cut-back. The near-field intensity profiles at the end-face of a 3 m length are shown in Fig. 5. The fundamental mode remains unchanged, while the doughnut mode has become slightly inhomogeneous. The loss for the LP_{01} mode is 0.11±0.02 dB/m, in good agreement with the data shown in Fig. 3(b) (0.13±0.01 dB/m). For the doughnut mode the loss was 0.23±0.04 dB/m, twice as high as for the LP_{01} mode. This can again be explained by stronger interactions with the glass cladding.

#101362 - $15.00 USD Received 8 Sep 2008; revised 17 Oct 2008; accepted 19 Oct 2008; published 21 Oct 2008

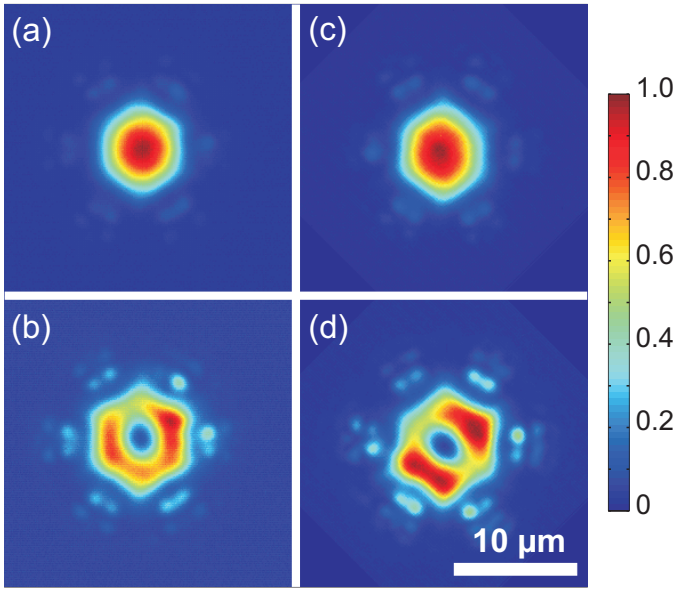

Fig. 5. Normalized mode intensity profiles measured at the end-face of a 19 m long HC-bandgap fiber: (a) fundamental LP_{01} mode; (b) LG_{01} mode; (c,d) the corresponding normalized intensity profiles after cut-back to 3 m of fiber.

4. Conclusions

Electronically generated holographic phase masks provide a versatile means of selectively exciting higher-order modes in HC-PCF, allowing purely electronic and completely reproducible adjustments to the launching conditions. We used the method to demonstrate excitation of higher-order modes up to LP_{31} in HC-kagome fibers. The reproducibility of the coupling allows comparative studies of the losses of fundamental and higher-order modes in both HC-bandgap and HC-kagome fibers. For both fiber types, losses for higher-order modes were observed to be larger than those of the fundamental mode.

The technique could be further improved by developing a routine for optimizing the coupling efficiency into higher-order modes. The best strategy here would be to limit the number of parameters that can be adjusted [22].

The results are relevant to applications in which the intensity distribution of the light inside the fiber is important, such as particle- or atom-guidance. Furthermore, higher-order modes have different values of group-velocity dispersion, so that adaptive coupling to them may be advantageous in optimizing nonlinear processes such as supercontinuum generation.

Acknowledgments

The authors express their gratitude to the Körber Foundation for the funding that made this project possible, and to Alexey Chugreev, Martin Garbos, and Silke Rammler for helping with the experiments.

#101362 - $15.00 USD Received 8 Sep 2008; revised 17 Oct 2008; accepted 19 Oct 2008; published 21 Oct 2008